

Reinforcement learning for the privacy preservation and manipulation of eye tracking data

Wolfgang Fuhl,¹ Efe Bozkir,¹ Enkelejda Kasneci,¹

¹ University Tübingen, Sand 14, 72076 Tübingen, Germany
wolfgang.fuhl@uni-tuebingen.de, efe.bozkir@uni-tuebingen.de, enkelejda.kasneci@uni-tuebingen.de

Abstract

In this paper, we present an approach based on reinforcement learning for eye tracking data manipulation. It is based on two opposing agents, where one tries to classify the data correctly and the second agent looks for patterns in the data, which get manipulated to hide specific information. We show that our approach is successfully applicable to preserve the privacy of the subjects. For this purpose, we evaluate our approach iteratively to showcase the behavior of the reinforcement learning based approach. In addition, we evaluate the importance of temporal, as well as spatial, information of eye tracking data for specific classification goals. In the last part of our evaluation, we apply the procedure to further public data sets without re-training the autoencoder or the data manipulator. The results show that the learned manipulation is generalized and applicable to unseen data as well.

Introduction

Due to the spread of the eye tracking technology over many fields (Fuhl 2019) and its use in everyday life, the specific information content in the eye tracking signal becomes more and more important (Bulling and Gellersen 2010; Majaranta and Bulling 2014; Eivazi et al. 2017b; Eivazi, Fuhl, and Kasneci 2017; Eivazi et al. 2017a; Bahmani et al. 2016; Fuhl et al. 2019a,c). This is mainly due to the fact that the gaze signal consists of very rich information and on the other hand that it cannot be turned off or consciously controlled by humans (Hansen et al. 2003; Stellmach and Dachsel 2012; Fuhl et al. 2016a, 2017b; Fuhl, Santini, and Kasneci 2017a; Fuhl et al. 2016b, 2017a, 2018b; Fuhl, Gao, and Kasneci 2020b; Fuhl, Santini, and Kasneci 2017b; Fuhl et al. 2018a). Many applications use this signal, however, still little value is placed on the anonymization of the signal. This is partly due to the fact that the topic of differential privacy has come into the focus of eye tracking research recently (Steil et al. 2019b,a; Liu et al. 2019), but also to the challenge of finding specific patterns in the signal makes a person identifiable.

Initially why the personal information should be protected in eye and gaze tracking applications along with the person specific patterns contained in the signals including age, gender, personal preference and health was mentioned by (Liebling and Preibusch 2014). This information poses a

new challenge to modern eye tracking systems, which is to hide this information. Differential privacy is one approach that achieves privacy of individuals' identities by adding randomly generated noise by keeping privacy-utility ratio acceptable. It usually works in case of prefabricated features; however, modern machine learning techniques such as convolutional neural networks (CNNs) are able to adapt their feature extractors. In addition, differential privacy is vulnerable to temporal correlations in the signals as independently generated noise can be helpful for the adversaries. As eye tracking data is temporally correlated in its nature, differential privacy approaches usually provide less privacy than claimed (Zhao, Zhang, and Poor 2017). Additionally, it would be more interesting to find specific patterns either in the stimulus or, as in this paper, in the scan path, which we can remove from the signal. This insight can be also used in many other areas gaze guidance (Latif et al. 2014; Kano and Tomonaga 2011) or expertise evaluation (Gegenfurtner, Lehtinen, and Säljö 2011; Kunze et al. 2013).

In this paper, we present an approach that is able to learn an image manipulation to hide specific information while preserving utility. Our approach uses reinforcement learning on the sparse representation learned by an autoencoder. This combination allows to manipulate general patterns in an image, since the autoencoder has to reconstruct it based on a reduced set of values. This reduced set can be found in the central part of the autoencoder. It is also called bottleneck, and the following transposed convolutions of the autoencoder reconstruct the image on the basis of the reduced set. Meaning that, those values represent patterns in an image that are manipulated by an agent in our approach. This agent tries to hide specific information by manipulating those values. Another agent tries to train new classifiers to adapt to the manipulated data. The retraining allows our approach to diminish personal patterns in the data since the classifiers adapt to the manipulated data. The main contributions of our work are as follows.

- 1 A novel approach to remove patterns from eye tracking data that contain personal information which achieves a similar goal as differential privacy.
- 2 Being independent of static features due to the iterative usage of CNNs.
- 3 Identification of general patterns in the data instead of

adding randomly generated noise as it is done in differential privacy.

- 4 Possibility of specifying the information type that should be hidden in the data.

Related Work

As we deal with two main topics including privacy using eye movements and reinforcement learning for manipulation of the eye tracking data, we organize this section accordingly.

Eye movements and privacy

The rich information content is available in human eye movements (Fuhl, Rong, and Enkelejda 2020; Fuhl et al. 2018c; Fuhl, Castner, and Kasneci 2018a,b; Fuhl and Kasneci 2018; Fuhl et al. 2019a,c; Fuhl, Gao, and Kasneci 2020a) and it has been shown in several studies. Cognitive load (Matthews et al. 1991), attention and personal interest in the scene (Hess and Polt 1960) can be extracted using pupil dilation. Mental disorders such as Alzheimer (Hutton, Nagel, and Loewenson 1984), Parkinson (Kuechenmeister et al. 1977), or schizophrenia (Holzman et al. 1974) can be detected using the eye movements as well. Additionally, the eye movements hold information about the activity of the human (Bulling, Weichel, and Gellersen 2013; Steil and Bulling 2015), the cognitive state (Marshall 2007) and personality traits (Hoppe et al. 2018). While all of this information is already critical, several researchers have shown that the gender and age can be also estimated from the eye movements (Cantoni et al. 2015; Sammaknejad et al. 2017). While these are useful for applications such as medical diagnosis or security, such information should not be available to everyone.

However, the high and unique information content in the eye tracking signal only becomes clear when biometrics applications are considered. Here, it is possible to unambiguously identify the person by means of the eye behavior. First, approaches required a moving point stimulus which was followed by the user (Kasprowski 2004; Kasprowski and Ober 2004, 2005) or static images (Maeder and Fookes 2003). Later, users were distinguished using eye movements with a task independent way (Bednarik et al. 2005). In addition, model based approaches using gaze behavior with oculomotor models were proposed (Komogortsev et al. 2010; Komogortsev and Holland 2013). Furthermore, distinguishing users while performing different tasks (Eberz et al. 2016) and a user authentication approach in virtual reality headsets (Zhang et al. 2018) were studied using eye movements.

These works show the potential threat to a human by revealing the gaze data. It also means that raw eye tracking data should be handled carefully, especially for storage and transmission purposes. However, there are not many works focusing on privacy-preserving eye tracking. An approach for head mounted eye trackers to detect privacy sensitive situations and to disable eye tracker first person camera using a mechanical shutter was proposed in (Steil et al. 2019b). Privacy-preserving gaze estimation using a randomized encoding based framework and replacing the iris textures of the eye images using rubber sheet model were studied in (Bozkir

et al. 2020b; Chaudhary and Pelz 2020), respectively. However, when the personal information protection is taken into account, differential privacy (Dwork et al. 2006) provides privacy with theoretical guarantees by adding randomly generated noise. While differential privacy guarantees that adversaries cannot infer whether an individual participated in a database, it also decreases the data utility due to the added noise. The privacy-utility trade-off is usually tailored around a specific use case (Pyrgelis, Troncoso, and De Cristofaro 2017), which can be understood as a classification target in the eye tracking world. Recently, differential privacy was applied to eye movements (Steil et al. 2019a; Bozkir et al. 2020a) and heatmaps (Liu et al. 2019) to protect privacy. Differential privacy is vulnerable to temporal correlations in the data and high dimensionality which are also validated by the recent work. As eye tracking data usually contains long recordings and it is high dimensional, it is challenging to provide the privacy while keeping the utility high. Our approach does not have exactly the same goal with differential privacy as we define a more relaxed version of privacy for eye tracking. With our approach, it is possible to specify the sensitive information that should be hidden in the data, which cannot be achieved with differential privacy.

Reinforcement learning

Reinforcement learning in the area of machine learning refers to one or more agents trying to learn a strategy that maximizes their reward (Kaelbling, Littman, and Moore 1996; Kober, Bagnell, and Peters 2013). The agent in this scenario has different actions that it can perform and after each action it receives a certain reward. For this, different cases have to be considered. The first case are temporal actions similar to a walk through a labyrinth where the agent receives his reward after it tried to go through the labyrinth (Kaelbling, Littman, and Moore 1996; Kober, Bagnell, and Peters 2013). This means that, after executing several actions, the agent receives the final reward. In the second case, the agent has several possible actions without temporal dependency (Kaelbling, Littman, and Moore 1996; Kober, Bagnell, and Peters 2013). In the following, we only deal with the temporally independent applications, because we also pursue this in this work.

In order to learn complex strategies, there are basically two approaches; one is model-based where a statistical model is given. This model is formulated as a Markov decision problem and is described by states and transitions that are known in advance. For the training of a model-based approach, a multitude of action selection strategy algorithms have been proposed. The first approach is called the greedy algorithm and usually used together with an optimistic initialization (Kaelbling, Littman, and Moore 1996; Kober, Bagnell, and Peters 2013). The second approach in reinforcement learning is called model free. In this approach, the algorithm learns strategies on how to behave under different circumstances. Therefore, the model is not known in advance, but estimated through exploration. The most famous approach is called the Q-learning algorithm (Luong et al. 2019). The Q-learning algorithm learns policies for, possibly, an infinite amount of states, where each state can

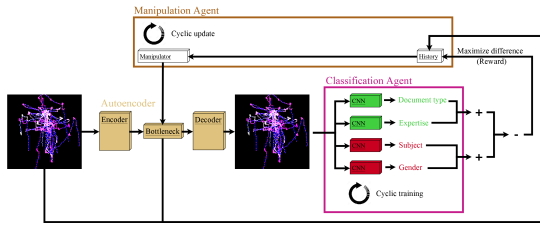


Figure 1: The workflow used for our approach. Classification Agent holds and uses the classifiers and Manipulation Agent the manipulator. Both agents are retrained after a fixed set of steps and have a buffer to hold old and new examples.

have different amount of actions. It consists of a learning rate and a table that holds the information gathered, the latter is updated with new observations. New actions are chosen using the same selection algorithms as in the model-based approaches. A disadvantage of the Q-learning algorithm is that it is only applicable if the state and action space is small. Therefore, the deep neural networks are employed to replace the table and output the best action by observing the current state. This is called the Deep Q-Learning algorithm (DQL) (Luong et al. 2019). In contrast to the tables, the DQL approach has the disadvantage that the neural networks are nonlinear function approximators that only receive the reward for training. This means that the network may not be stable or even diverge (Mnih et al. 2015). To solve this issue, multiple approaches have been proposed and combined (Luong et al. 2019). The first is called the experience replay mechanism. For this approach, the algorithm initializes a replay memory and the initialization is done using the ϵ -greedy algorithm. Out of this memory, mini batches are selected and used for training. Afterwards, the neural network is used to make new experiences, which are stored in the memory. Therefore, the network can always learn on old and new experiences and is thus, stable to train (Luong et al. 2019). The second approach to stabilize the training of the neural network is called fixed target Q-network. For this approach, two neural networks are used. The first one is trained based on the memory and then used to slowly update the second network after a fixed set of steps of the learning process (Luong et al. 2019). This is especially helpful if the initial exploration is not sufficient.

Method

Figure 1 shows the general workflow of our approach. The autoencoder is trained preliminary to reconstruct the image. In its central part, it holds values that correspond to general patterns for the reconstruction of the image (Bottleneck in Figure 1). The idea behind using the autoencoder is that it reduces the input data ($64 * 64 * 3 = 12.228$ to $4 * 4 * 256 = 4096$) and, thus, the possible action combinations of the Manipulation Agent as well. Furthermore, in the end it ensures that an image is still generated that is similar to the input image or it consists of general patterns compared to a direct manipulation of the image by the Manipulation

Agent. The Manipulation Agent is the reinforcement part of our approach. It learns a manipulation of the bottleneck from the autoencoder based on the previously seen input images and the classification result from Classification Agent. This classification result is only the difference between the good and the bad (Green and red classifiers in Figure 1, respectively) information revealed by the classifiers. The difference is used as a reward in the Manipulation Agent for the performed manipulation, whereas the image itself is the state. The different classification objectives (Document type, expertise, subject, gender) in Figure 1 are intended to indicate that our approach supports any number of classifiers. The Manipulation Agent tries to worsen the accuracy of the red classifiers and to keep the accuracy of the green classifiers high. In contrast, the Classification Agent tries to adapt the classifiers to the new image manipulation by retraining them. In the following each part is described in detail.

The first column of Table 1 shows the architecture of the used autoencoder. Each convolution block is followed by a rectifier linear unit (ReLU) and max pooling for size reduction. For the decoder of the autoencoder, we used transposed convolutions instead of pooling. The input to the network is an image with size $64 * 64 * 3$. The bottleneck in the autoencoder is the block with size $4 * 4 * 256$. For the training, we used stochastic gradient decent (SGD) with an initial learning rate of 10^{-2} , decreasing each 200 epochs by a factor of 10^{-1} . The training stops at a learning rate of 10^{-7} . Weight decay and momentum were to $5 * 10^{-4}$ and $9 * 10^{-1}$, respectively. During the training, we used a batch size of 40 and the L2 loss formulation. The autoencoder is trained only once before starting our reinforcement learning approach.

The classifiers in the Classification Agents use a similar structure as the autoencoder and details of Classifier A and B are depicted in Table 1 second and third columns, respectively. Each convolution block uses a ReLU together with a max pooling operation. Before the first fully connected layer, we used a dropout, which deactivates 50% randomly. Classifiers A and B in Table 1 have the same structure except for the last fully connected layer, which has either eight (Subject) or four (Stimulus image) output neurons. For the training, we used SGD with an initial learning rate of 10^{-4} decreasing each 500 epochs by a factor of 10^{-1} . The training stops at a learning rate of 10^{-7} . Weight decay and momentum were set to $5 * 10^{-4}$ and $9 * 10^{-1}$, respectively. During training, we used a batch size of 50 and the log multi-class loss with softmax.

Since these classifiers are subject to the cyclic training of the Classification Agent, they are always re-trained once the reinforcement learning has been stabilized. This new training is done with random initialization. The idea behind is that the convolutions, which learn new feature extractors, adapt to the new image manipulation and, thus, improve the classification result. The training itself is done using all the manipulated images seen so far in addition to the non-manipulated ones (only from the training set).

We show the workflow for the Classification Agent with the memory in Figure 2. In comparison to Figure 1, which is a general overview, it can be seen that we now have only two classes. Those two classes are also used in our experiments

Table 1: The configurations of the used models in our work. The autoencoder is used for extracting high level features from the input image. Classifier A and Classifier B are the networks to classify the subject and stimulus image, respectively. The DQL model is used in the Manipulation Agent as Deep Q-Learning algorithm (DQL).

Autoencoder	Classifier A	Classifier B	DQL
Input $64 \times 64 \times 3$	$64 \times 64 \times 3$	$64 \times 64 \times 3$	$64 \times 64 \times 3$
CONV $32 \times 7 \times 7$	$32 \times 7 \times 7$	$32 \times 7 \times 7$	$32 \times 7 \times 7$
ReLu, Max Pooling	ReLu, Max Pooling	ReLu, Max Pooling	ReLu, Max Pooling
CONV $64 \times 7 \times 7$	$64 \times 7 \times 7$	$64 \times 7 \times 7$	$64 \times 7 \times 7$
ReLu, Max Pooling	ReLu, Max Pooling	ReLu, Max Pooling	ReLu, Max Pooling
CONV $128 \times 5 \times 5$	$128 \times 5 \times 5$	$128 \times 5 \times 5$	$128 \times 5 \times 5$
ReLu, Max Pooling	ReLu, Max Pooling	ReLu, Max Pooling	ReLu, Max Pooling
CONV $256 \times 5 \times 5$	$256 \times 5 \times 5$	$256 \times 5 \times 5$	Fully 4096
ReLu	ReLu, Max Pooling	ReLu, Max Pooling	-
TCONV $128 \times 5 \times 5$	Fully 512	Fully 512	-
ReLu	ReLu	ReLu	-
TCONV $64 \times 5 \times 5$	Fully #Classes	Fully #Classes	-
ReLu	-	-	-
TCONV $32 \times 7 \times 7$	-	-	-
ReLu	-	-	-
TCONV $3 \times 7 \times 7$	-	-	-

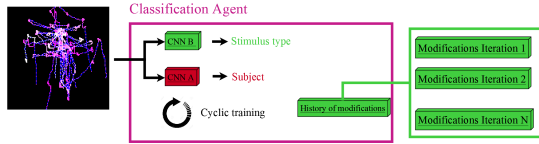


Figure 2: The setup of the Classification Agent with a memory for manipulated data seen in the past.

for the evaluation section which is why we decided to insert them in the detailed view of the Classification Agent. In the memory (Figure 2) are all the seen manipulated images from the training set together with their labels. Images from the validation set are discarded and, therefore, not stored in the memory of the Classification Agent. For the training and test sets, we made a 50% to 50% split. We separated the data to produce an equal amount of stimulus and subject classes. As it can be seen, Classification Agent does not use reinforcement learning. This agent can be understood as a supervised learner, which retrains its classifiers.

In contrast to the Classification Agent, the Manipulation Agent uses reinforcement learning for training. The used DQL model is shown in the fourth column of the Table 1. It consists of three convolution blocks and a fully connected output layer. The input of this model is the current image, which is called the state, and the output (4096 fully connected neurons) are the actions. Between each convolution block, we used ReLu and max pooling as in the previous models. The output of the last layer was set to 1 if it was greater or equal to 0.5. Otherwise it was set to 0, meaning that our model could either deactivate a feature in the bottleneck of the autoencoder or let it unchanged. For the training, we used SGD with a fixed learning rate of 10^{-4} . The training stops after 10 epochs of training on the entire memory of the Manipulation Agent. Weight decay and momentum were set

to 1×10^{-5} and 9×10^{-1} , respectively. During the training, we used a batch size of 100 and the L2 loss formulation for reinforcement learning $(predicted - actual)^2$. The parameter *predicted* in this context means the result of DQL1 from the current input image. Since there is no ground truth in reinforcement learning, the parameter *actual* is computed based on a second network (DQL2) and the reward R . Therefore, the ground truth is formulated as $actual = R + \gamma * DQL2$. As mentioned before, R is the reward (Result of Classification Agent), $DQL2$ is the output of a second network and γ is the discount factor, which is adjusted through training so that the network explores more in the beginning. This usage of two neural networks is called a fixed target Q-network (Luong et al. 2019). Therefore, after 10 training runs of DQL1, we set $DQL2 = DQL1$ since DQL1 had stabilized.

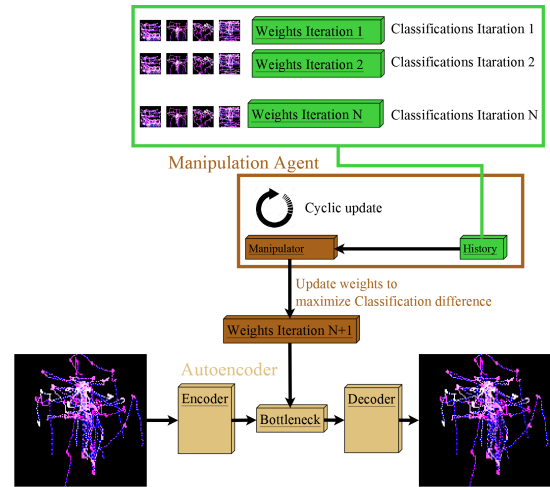


Figure 3: The memory and setup of the Manipulation Agent.

In addition to the fixed target network, we use the experience replay mechanism (Luong et al. 2019) as can be seen in Figure 3. As mentioned in the related work, this concept describes the memory which holds all examples (Stimulus, actions, and classification result). In the memory, we only store examples from the training set, since we want to evaluate our approach especially for unseen data. The memory is initialized before starting the entire approach and the networks DQL1 and DQL2 are trained on it. For this initialization, we compute the change of each value in the bottleneck on the classification and store it in the memory of the Manipulation Agent. In addition, we compute 100 random changes of 2-100 values in the bottleneck. This means that for the change of two values, we compute 100 random changes and the same for three values, four values, and so on.

For data augmentation of all models, we used random noise which was in the range of 0-20%, cropping and shifting the scanpath. Cropping means the extraction of the 60-100% of the scanpath randomly and drawing it on the input image. Shifting means randomly selected constant shift of the entire scanpath, where we selected in the range of 0-30% of the stimulus size.

In addition to our reinforcement learning approach, we have evaluated differential privacy particularly in terms of utility and a Generative Adversarial Network (GAN) namely a supervised approach to justify the usage of reinforcement learning for the manipulation. While our approach does not provide formal privacy guarantees as differential privacy and we provide more relaxed version of privacy while keeping the utility high, differential privacy is also vulnerable, especially to the correlated and high dimensional data. Therefore, differential privacy, in our context, provides less privacy compared to applications in the domain of databases (Zhao, Zhang, and Poor 2017). For evaluation, we opted for the standard Laplacian mechanism of the ϵ -Differential Privacy (ϵ -DP) applied both on raw eye tracking data (DP-Raw) and generated image (DP-Image) (Dwork et al. 2006; Sarathy and Muralidhar 2011). In the differential privacy, the amount of added noise is generated using function sensitivities (Δf) and an ϵ parameter. For the function sensitivities, we used L_1 sensitivities which are calculated as the maximum Manhattan distance between recordings (Rastogi and Nath 2010) and maximum pixel distance per each channel of the images for DP-Raw and DP-Image, respectively. N -sized randomly generated Laplacian noise vectors are calculated as $Lap^N(\lambda) = Lap^N(\Delta f/\epsilon)$, where N denotes size of the noise added data. For the evaluation, we applied the Laplacian mechanism 100 times and averaged the results accordingly. We used majority voting while selecting the detected class by the networks. To find the optimal utility-privacy ratio, we evaluated various ϵ values in the search range of $[0.01 - 15.0]$ and $[10.00 - 500.0]$ by 0.01 sized steps for the images and raw gaze data, respectively. For the images, the ϵ values are multiplied by the image resolution (64×64) as the differential privacy is preserved by the Sequential Composition Theorem due to the independence of the image pixels (McSherry 2009). Therefore, the search range for the ϵ was $[40.96 - 61440]$, but the 0.01 search steps are made based on the single pixel search range

($[0.01 - 15.0]$). We skipped ϵ values for the raw eye tracking data if there were less than three gaze points remaining on the image. The optimal ϵ was selected based on the maximum distance between the stimulus and subject classification, where the subject classification was at chance level.

In addition, we have evaluated a supervised learning approach to justify the usage of reinforcement learning. The same models as shown in Table 1 were used and trained as a GAN. The autoencoder is used as the generator, whereas the Classifiers A and B are used as discriminators. Before we trained the GAN, we initially trained the Autoencoder, Classifier A, and Classifier B for 100 epochs with the already provided training parameters. This was done to stabilize the training of the GAN afterwards. To adapt the initial training to the training of the GAN, we added the logarithmic loss from the generated image as was done in (Goodfellow et al. 2014) with the difference that the classifiers still had to predict the correct class.

For the generator (G), we used the formulation of ($\log(1 - D(G(I)))$) (Goodfellow et al. 2014) but in our case the discriminator (D) consists of two networks. Therefore, Classifier A and Classifier B can only contribute 0.5 each but in inverse directions. This means that if Classifier A is correct, it contributes 0.5 and if Classifier B is wrong then it additionally contributes 0.5 since we want the GAN to learn to preserve the information classified by the Classifier A and hide the information important for the Classifier B. Based on the softmax output, we simply compute the probability for the correct class for the Classifiers A and B and weight them both with 0.5.

Evaluation

In this section, we give an overview on the used datasets and discuss our results.

Datasets

ETRA 2019 Challenge dataset (Otero-Millan et al. 2008; McCamy et al. 2014): A dataset with 8 subjects and 120 trials per subject. Therefore, it consists of 960 trials with a length of 45 seconds per trial. The dataset includes different tasks, namely, visual fixation, visual search, and visual exploration. Additionally, four different stimuli were presented; which are blank, natural, where is waldo, and picture puzzle. For the image generation, out of the raw gaze data files, we used the approach from (Fuhl et al. 2019b). This means that the raw gaze data is in the red channel as dots, the green channel holds the time by adjusting the intensity of the dot, and the blue channel holds the relationship of the gaze points by connecting them as lines, which can be seen in Figure 4.

Gaze (Dorr et al. 2010): A data set with eye tracking data on dynamic scenes. The data was recorded using an SR Research EyeLink II eye tracker with 250 Hz. For our experiment, we used the data provided for static images where each static image of a video was considered the same image. In addition, we excluded subject V01 since there was only one recording available. Therefore, we used the eye tracking data of 10 subjects on 9 images for our experiment with an

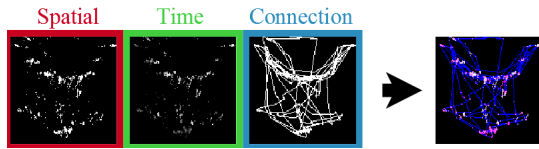


Figure 4: The encoding of eye tracking data as image.

average recording length of 2 seconds. The training and test split was done using 50% for the training and 50% for the validation with a random selection. To treat both classifiers equally, the training set contained data from each subject and image.

WherePeopleLook (Judd et al. 2009) (WPL): An eye tracking dataset for integrating top-down features into saliency map generation. It consists of 1003 static images with eye tracking data of 15 subjects per image with an average recording length of 3 seconds. For our experiment, we used a 50%-50% split where the training data included all subjects and images at least once to treat both classifiers equally.

DOVES (Bovik et al. 2009): An eye tracking dataset of 29 subjects on 101 natural images with an average recording length of 5 seconds. The recordings were performed with a 200 Hz high-precision dual-Purkinje eye tracker. Similar to the WherePeopleLook (Judd et al. 2009) dataset, we made a 50%-50% training and test split. The training data included each subject and image at least once to treat both classifiers equally.

Results

For our first two experiments, we used the ETRA 2019 Challenge dataset. The first experiment shows the results of our approach for different iterations, as well as before and after the adaption of the classifiers (Classification Agent). This experiment shows that our approach is capable of removing unwanted information in the scanpath. In this scenario, it is the information of the subject. Table 2 shows the classification results per iteration. With iteration, we mean that the reinforcement learning (RL), namely the Manipulation Agent has stabilized, which are approximately 1000 training runs. After each iteration, the Classification Agent starts to retrain the classifiers, which is indicated by the adaption rows. RL-Initial in Table 2 corresponds to the initial results of the pretrained classifiers. The chance level is shown at the bottom of Table 2. As can be seen, the Manipulation Agent always succeeds in dropping the classification accuracy for the subject close to the chance level. Afterwards, the Classification Agent adapts the classifiers, but with less success for the subject classification if the process over all iterations is considered. In the last iteration (20), the training of the subject classifier fails and is close to the chance level. This is also the case for DP-Raw (Differential privacy applied to the raw eye tracking data), DP-Image (Differential privacy applied to the image), and the GAN (Generative Adversarial Network) approach. It is clear that our reinforcement learning approach performs better than differential privacy in terms of receiving the stimulus information, namely

Table 2: Accuracy of the classifiers after each iteration and before as well as after the adaption of Classification Agent. RL is the proposed approach, GAN is the same models trained supervised, DP-Raw is the Differential Privacy applied to the raw gaze data, and DP-Image is the differential privacy applied to the image. The best results are in bold.

Iteration	No Adaption		Adaption	
	Stim	Sub	Stim	Sub
RL-Initial	-	-	0.96	0.93
RL-1	0.95	0.13	0.96	0.93
RL-2	0.95	0.11	0.95	0.91
RL-5	0.91	0.12	0.93	0.52
RL-10	0.88	0.14	0.91	0.31
RL-15	0.78	0.12	0.86	0.22
RL-20	0.81	0.13	0.83	0.15
GAN	0.75	0.13	0.81	0.15
DP-Raw $\epsilon = 238.83$	0.27	0.15	0.30	0.15
DP-Image $\epsilon = 10485.76$	0.41	0.11	0.59	0.15
Chance level	0.25	0.12	0.25	0.12

the utility. In addition, our approach performs slightly better than the GAN approach.

In the second experiment, we evaluate the importance of different channels of the input image for different iterations of our approach. This experiment shows the advantage of our approach to other privacy preservation methods since the feature extractors (Neural networks in the Classification Agent) adapt to the new image manipulation as well as our image manipulation technique. For all experiments, we used a 50% split of the data where the test and validation set contain always equal amount of subjects and stimuli samples. Table 3 shows the percentage amount of changed values per channel normalized over the total amount of changed values. Due to the construction of the image with raw dots in the red channel, connected dots in the blue channel, and the time as intensity value per dot in the green channel, we estimated the importance of their contribution. For iteration 1, it can be seen that the subject information was mainly extracted out of the red channel, which holds only spatial information. In the second iteration, this swaps to the blue channel, which holds the interconnections between the gaze points and, therefore, the spatial information. After 5 iterations, the amount of changes have balanced per channel. If we compare these results to Table 2, it can be seen that it had already a significant impact on the adaption of the subject classifier. After the last iteration, the amount of changes has again nearly balanced, where the green channel is the lowest. Since the green channel is the only channel that has temporal information, it could be argued that it is less important for the subject information since the green channel also contains spatial information. This statement is purely hypothetical and requires further experiments and research as well as another construction of input data.

In the third experiment, we use the data manipulation (learned with reinforcement learning) and the autoencoder on other public data sets without further training. However,

Table 3: Importance of spatial (R, B; red and blue channel) and temporal (G; intensity in green channel) features for the classification per iteration. The importance is measured in percentage of values changed in total per channel.

Iteration	Red (Spat.)	Green (Temp.)	Blue (Spat.)
1	72%	16%	12%
2	19%	12%	69%
5	36%	33%	31%
10	41%	20%	39%
15	38%	22%	40%
20	37%	28%	35%

the classifiers are re-trained on the output of the autoencoder and additionally adapted to the data manipulation in the further step. For the classification on the datasets Gaze, WherePeopleLook, and DOVES, we used the same model as in Experiment 1 (Table 1). For training, we set the initial learning rate to 10^{-2} and reduced it by a factor of 10^{-1} every 100 epochs until we reached 10^{-7} . The optimizer used was SGD with weight decay of $5 * 10^{-4}$ and momentum of 0.9. For the dataset Gaze, we used a batch size of twice the number of classes and made sure that there were always 2 examples of each class in a batch. For the WherePeopleLook, we used double the number of classes for the subject classification as well. For the Stimulus Classification, we used only the single class number as batch size. For the DOVES dataset, we used twice the number of classes as batch size for both classifiers as for the Gaze dataset and made sure that there were always two examples of each class per batch as well.

Table 4 shows the results of the third experiment. The results without the data manipulation are depicted in the first column. Comparing these with the results on the Challenge dataset in Table 2, it is seen that the results are significantly lower. One of the reasons is that there are more number of classes which increases the challenge for the classification, but the main reason is the significantly lower recording time. For the Challenge data set, the average recording time is 45 seconds. In comparison, Gaze, WherePeopleLook, and DOVES datasets have an average of 2, 3, and 5 seconds, respectively. This shows that the Challenge dataset provides a multiple of the information for the neural networks. It means that the data from the Challenge dataset contains significantly more personal information as well as more information about the structure of the stimuli. It is also interesting how little eye tracking data is sufficient to classify a subject. For instance, if the results of the DOVES dataset are compared with Gaze and WherePeopleLook datasets, it is seen in the first column of Table 4 that DOVES has a higher accuracy for the subject classification although it has a lower chance level, but a 2-3 seconds longer recording time. In contrast, the detection rate for the stimuli classification is significantly lower compared to the other datasets.

The results after the data manipulation by the Manipulation Agent are shown in the second column of Table 4. The Manipulation Agent has not been retrained and neither has

Table 4: Accuracy on new unseen datasets with retrained classifiers but the same data manipulation learned from experiment 1 and 2 as well as the same weights for the autoencoder. RL is the proposed approach, GAN is the same models trained supervised, DP-Raw is the differential privacy applied to the raw gaze data, and DP-Image is the differential privacy applied to the image. The best results are in bold.

Data	Method	None		Manipulation		Adapted	
		Stim	Sub	Stim	Sub	Stim	Sub
Gaze	RL			40	8.88	71.11	13.33
	GAN			37.24	14.32	61.64	19.53
	DP-Raw $\epsilon = 32.85$	75	31.66	15.44	12.54	16.25	13.96
	DP-Image $\epsilon = 34938.88$			21.22	11.81	59.83	13.61
	Chance	11.11	10	11.11	10	11.11	10
WPL	RL			21.54	6.39	30.48	8.28
	GAN			18.47	14.76	26.74	20.37
	DP-Raw $\epsilon = 73.66$	31.23	30.06	0.19	7.09	0.4	8.93
	DP-Image $\epsilon = 16547.84$			7.15	6.72	8.41	8.91
	Chance	0.099	6.66	0.099	6.66	0.099	6.66
DOVES	RL			4.3	6.69	9.15	13.66
	GAN			5.68	6.73	8.26	19.55
	DP-Raw $\epsilon = 438.15$	10.86	44.90	1.81	3.95	1.42	12.45
	DP-Image $\epsilon = 13762.56$			1.14	5.01	1.5	22.11
	Chance	0.99	3.44	0.99	3.44	0.99	3.44

the autoencoder. As it is shown in the results, the data manipulation has a significant impact on the accuracy of the classifiers. It holds for the stimulus and subjects, although the subject classification is influenced more, except for the DOVES dataset as everything is reduced below the chance level. Since this can be purely due to data augmentation, we have also adapted the classifiers to the data manipulation via training. For this purpose, the training examples were manipulated with the Manipulation Agent and both the unaltered and the manipulated data were used for the training. The results are be shown in the third column of Table 4. While the subject classification in the DOVES dataset is still significantly above the chance level with 13.66%, the personal information was mainly removed in the other two datasets. The stimulus information was mainly retained for all datasets which empirically shows that it is possible to find generalized patterns to hide specific information using our approach.

Conclusion

In this work, we showed the applicability of reinforcement learning for removing personal information from eye tracking data. In addition, it can be used to evaluate the features and is able to adapt to an adaptive attacker. Our approach

is able to remove and preserve information of multiple classification targets. We empirically showed that our approach has generalized and is also applicable to unseen data sets. This is interesting since it could mean that our approach can be applied to improve the robustness of neural networks as a pre-processing module or during training as an adversarial attack generator.

References

- Bahmani, H.; Fuhl, W.; Gutierrez, E.; Kasneci, G.; Kasneci, E.; and Wahl, S. 2016. Feature-based attentional influences on the accommodation response. In *Vision Sciences Society Annual Meeting Abstract*.
- Bednarik, R.; Kinnunen, T.; Mihaila, A.; and Fränti, P. 2005. Eye-movements as a biometric. In *Scandinavian conference on image analysis*, 780–789. Springer.
- Bovik, A.; Cormack, L.; Van Der Linde, I.; and Rajashekar, U. 2009. DOVES: a database of visual eye movements. *Spatial vision* 22(2): 161–177.
- Bozkir, E.; Günlü, O.; Fuhl, W.; Schaefer, R. F.; and Kasneci, E. 2020a. Differential Privacy for Eye Tracking with Temporal Correlations.
- Bozkir, E.; Ünal, A. B.; Akgün, M.; Kasneci, E.; and Pfeifer, N. 2020b. Privacy Preserving Gaze Estimation Using Synthetic Images via a Randomized Encoding Based Framework. In *ACM Symposium on Eye Tracking Research and Applications*, ETRA '20 Short Papers. New York, NY, USA: Association for Computing Machinery. ISBN 9781450371346. doi:10.1145/3379156.3391364.
- Bulling, A.; and Gellersen, H. 2010. Toward mobile eye-based human-computer interaction. *IEEE Pervasive Computing* 9(4): 8–12.
- Bulling, A.; Weichel, C.; and Gellersen, H. 2013. EyeContext: recognition of high-level contextual cues from human visual behaviour. In *Proceedings of the sigchi conference on human factors in computing systems*, 305–308. ACM.
- Cantoni, V.; Galdi, C.; Nappi, M.; Porta, M.; and Riccio, D. 2015. GANT: Gaze analysis technique for human identification. *Pattern Recognition* 48(4): 1027–1038.
- Chaudhary, A. K.; and Pelz, J. B. 2020. Privacy-Preserving Eye Videos Using Rubber Sheet Model. In *ACM Symposium on Eye Tracking Research and Applications*, ETRA '20 Short Papers. New York, NY, USA: Association for Computing Machinery. ISBN 9781450371346. doi:10.1145/3379156.3391375.
- Dorr, M.; Martinetz, T.; Gegenfurtner, K. R.; and Barth, E. 2010. Variability of eye movements when viewing dynamic natural scenes. *Journal of vision* 10(10): 28–28.
- Dwork, C.; McSherry, F.; Nissim, K.; and Smith, A. 2006. Calibrating Noise to Sensitivity in Private Data Analysis. In Halevi, S.; and Rabin, T., eds., *Theory of Cryptography*, 265–284. Berlin, Heidelberg: Springer Berlin Heidelberg.
- Eberz, S.; Rasmussen, K. B.; Lenders, V.; and Martinovic, I. 2016. Looks like eve: Exposing insider threats using eye movement biometrics. *ACM Transactions on Privacy and Security (TOPS)* 19(1): 1.
- Eivazi, S.; Fuhl, W.; and Kasneci, E. 2017. Towards Intelligent Surgical Microscopes: Surgeons Gaze and Instrument Tracking. In *Proceedings of the 22st International Conference on Intelligent User Interfaces, IUI 2017*. ACM.
- Eivazi, S.; Hafez, A.; Fuhl, W.; Afkari, H.; Kasneci, E.; Lehecka, M.; and Bednarik, R. 2017a. Optimal eye movement strategies: a comparison of neurosurgeons gaze patterns when using a surgical microscope. *Acta Neurochirurgica*.
- Eivazi, S.; Slupina, M.; Fuhl, W.; Afkari, H.; Hafez, A.; and Kasneci, E. 2017b. Towards automatic skill evaluation in microsurgery. In *Proceedings of the 22st International Conference on Intelligent User Interfaces, IUI 2017*. ACM.
- Fuhl, W. 2019. *Image-based extraction of eye features for robust eye tracking*. Ph.D. thesis, University of Tübingen.
- Fuhl, W.; Bozkir, E.; Hosp, B.; Castner, N.; Geisler, D.; C., T.; and Kasneci, E. 2019a. Encodji: Encoding Gaze Data Into Emoji Space for an Amusing Scanpath Classification Approach ;). In *Eye Tracking Research and Applications*.
- Fuhl, W.; Bozkir, E.; Hosp, B.; Castner, N.; Geisler, D.; Santini, T. C.; and Kasneci, E. 2019b. Encodji: Encoding Gaze Data Into Emoji Space for an Amusing Scanpath Classification Approach ;). In *Eye Tracking Research and Applications*.
- Fuhl, W.; Castner, N.; and Kasneci, E. 2018a. Histogram of oriented velocities for eye movement detection. In *International Conference on Multimodal Interaction Workshops, ICMIW*.
- Fuhl, W.; Castner, N.; and Kasneci, E. 2018b. Rule based learning for eye movement type detection. In *International Conference on Multimodal Interaction Workshops, ICMIW*.
- Fuhl, W.; Castner, N.; Kübler, T. C.; Lotz, A.; Rosenstiel, W.; and Kasneci, E. 2019c. Ferns for area of interest free scanpath classification. In *Proceedings of the 2019 ACM Symposium on Eye Tracking Research & Applications (ETRA)*.
- Fuhl, W.; Eivazi, S.; Hosp, B.; Eivazi, A.; Rosenstiel, W.; and Kasneci, E. 2018a. BORE: Boosted-oriented edge optimization for robust, real time remote pupil center detection. In *Eye Tracking Research and Applications, ETRA*.
- Fuhl, W.; Gao, H.; and Kasneci, E. 2020a. Neural networks for optical vector and eye ball parameter estimation. In *ACM Symposium on Eye Tracking Research & Applications, ETRA 2020*. ACM.
- Fuhl, W.; Gao, H.; and Kasneci, E. 2020b. Tiny convolution, decision tree, and binary neuronal networks for robust and real time pupil outline estimation. In *ACM Symposium on Eye Tracking Research & Applications, ETRA 2020*. ACM.
- Fuhl, W.; Geisler, D.; Santini, T.; Appel, T.; Rosenstiel, W.; and Kasneci, E. 2018b. CBF: Circular binary features for robust and real-time pupil center detection. In *ACM Symposium on Eye Tracking Research & Applications*.

- Fuhl, W.; and Kasneci, E. 2018. Eye movement velocity and gaze data generator for evaluation, robustness testing and assess of eye tracking software and visualization tools. In *Poster at Egocentric Perception, Interaction and Computing, EPIC*.
- Fuhl, W.; Kübler, T. C.; Hospach, D.; Bringmann, O.; Rosenstiel, W.; and Kasneci, E. 2017a. Ways of improving the precision of eye tracking data: Controlling the influence of dirt and dust on pupil detection. *Journal of Eye Movement Research* 10(3).
- Fuhl, W.; Rong, Y.; and Enkelejda, K. 2020. Fully Convolutional Neural Networks for Raw Eye Tracking Data Segmentation, Generation, and Reconstruction. In *Proceedings of the International Conference on Pattern Recognition*, 0–0.
- Fuhl, W.; Santini, T.; Geisler, D.; Kübler, T. C.; and Kasneci, E. 2017b. EyeLad: Remote Eye Tracking Image Labeling Tool. In *12th Joint Conference on Computer Vision, Imaging and Computer Graphics Theory and Applications (VISIGRAPP 2017)*.
- Fuhl, W.; Santini, T.; Geisler, D.; Kübler, T. C.; Rosenstiel, W.; and Kasneci, E. 2016a. Eyes Wide Open? Eyelid Location and Eye Aperture Estimation for Pervasive Eye Tracking in Real-World Scenarios. In *ACM International Joint Conference on Pervasive and Ubiquitous Computing: Adjunct publication – PETMEI 2016*.
- Fuhl, W.; Santini, T.; and Kasneci, E. 2017a. Fast and Robust Eyelid Outline and Aperture Detection in Real-World Scenarios. In *IEEE Winter Conference on Applications of Computer Vision (WACV 2017)*.
- Fuhl, W.; Santini, T.; and Kasneci, E. 2017b. Fast camera focus estimation for gaze-based focus control. In *CoRR*.
- Fuhl, W.; Santini, T.; Kuebler, T.; Castner, N.; Rosenstiel, W.; and Kasneci, E. 2018c. Eye movement simulation and detector creation to reduce laborious parameter adjustments. *arXiv preprint arXiv:1804.00970*.
- Fuhl, W.; Santini, T.; Reichert, C.; Claus, D.; Herkommer, A.; Bahmani, H.; Rifai, K.; Wahl, S.; and Kasneci, E. 2016b. Non-Intrusive Practitioner Pupil Detection for Unmodified Microscope Oculars. *Elsevier Computers in Biology and Medicine* 79: 36–44.
- Gegenfurtner, A.; Lehtinen, E.; and Säljö, R. 2011. Expertise differences in the comprehension of visualizations: A meta-analysis of eye-tracking research in professional domains. *Educational Psychology Review* 23(4): 523–552.
- Goodfellow, I.; Pouget-Abadie, J.; Mirza, M.; Xu, B.; Warde-Farley, D.; Ozair, S.; Courville, A.; and Bengio, Y. 2014. Generative adversarial nets. In *Advances in neural information processing systems*, 2672–2680.
- Hansen, J. P.; Johansen, A. S.; Hansen, D. W.; Itoh, K.; and Mashino, S. 2003. Command without a click: Dwell time typing by mouse and gaze selections. In *Proceedings of Human-Computer Interaction–INTERACT*, volume 3, 121–128.
- Hess, E. H.; and Polt, J. M. 1960. Pupil size as related to interest value of visual stimuli. *Science* 132(3423): 349–350.
- Holzman, P. S.; Proctor, L. R.; Levy, D. L.; Yasillo, N. J.; Meltzer, H. Y.; and Hurt, S. W. 1974. Eye-tracking dysfunctions in schizophrenic patients and their relatives. *Archives of general psychiatry* 31(2): 143–151.
- Hoppe, S.; Loetscher, T.; Morey, S. A.; and Bulling, A. 2018. Eye Movements During Everyday Behavior Predict Personality Traits. *Frontiers in Human Neuroscience* 12: 105. ISSN 1662-5161. doi:10.3389/fnhum.2018.00105.
- Hutton, J. T.; Nagel, J.; and Loewenson, R. B. 1984. Eye tracking dysfunction in Alzheimer-type dementia. *Neurology* 34(1): 99–99.
- Judd, T.; Ehinger, K.; Durand, F.; and Torralba, A. 2009. Learning to Predict Where Humans Look. In *IEEE International Conference on Computer Vision (ICCV)*.
- Kaelbling, L. P.; Littman, M. L.; and Moore, A. W. 1996. Reinforcement learning: A survey. *Journal of artificial intelligence research* 4: 237–285.
- Kano, F.; and Tomonaga, M. 2011. Perceptual mechanism underlying gaze guidance in chimpanzees and humans. *Animal cognition* 14(3): 377–386.
- Kasprowski, P. 2004. Human identification using eye movements. *Institute of Computer Science*.
- Kasprowski, P.; and Ober, J. 2004. Eye movements in biometrics. In *International Workshop on Biometric Authentication*, 248–258. Springer.
- Kasprowski, P.; and Ober, J. 2005. Enhancing eye-movement-based biometric identification method by using voting classifiers. In *Biometric Technology for Human Identification II*, volume 5779, 314–323. International Society for Optics and Photonics.
- Kober, J.; Bagnell, J. A.; and Peters, J. 2013. Reinforcement learning in robotics: A survey. *The International Journal of Robotics Research* 32(11): 1238–1274.
- Komogortsev, O. V.; and Holland, C. D. 2013. Biometric authentication via complex oculomotor behavior. In *2013 IEEE Sixth International Conference on Biometrics: Theory, Applications and Systems (BTAS)*, 1–8. IEEE.
- Komogortsev, O. V.; Jayarathna, S.; Aragon, C. R.; and Mahmoud, M. 2010. Biometric identification via an oculomotor plant mathematical model. In *Proceedings of the 2010 Symposium on Eye-Tracking Research & Applications*, 57–60. ACM.
- Kuechenmeister, C. A.; Linton, P. H.; Mueller, T. V.; and White, H. B. 1977. Eye tracking in relation to age, sex, and illness. *Archives of General Psychiatry* 34(5): 578–579.
- Kunze, K.; Kawaichi, H.; Yoshimura, K.; and Kise, K. 2013. Towards inferring language expertise using eye tracking. In *CHI'13 Extended Abstracts on Human Factors in Computing Systems*, 217–222. ACM.

- Latif, N.; Gehmacher, A.; Castelhana, M. S.; and Munhall, K. G. 2014. The art of gaze guidance. *Journal of experimental psychology: human perception and performance* 40(1): 33.
- Liebling, D. J.; and Preibusch, S. 2014. Privacy considerations for a pervasive eye tracking world. In *Proceedings of the 2014 ACM International Joint Conference on Pervasive and Ubiquitous Computing: Adjunct Publication*, 1169–1177. ACM.
- Liu, A.; Xia, L.; Duchowski, A.; Bailey, R.; Holmqvist, K.; and Jain, E. 2019. Differential privacy for eye-tracking data. *arXiv preprint arXiv:1904.06809*.
- Luong, N. C.; Hoang, D. T.; Gong, S.; Niyato, D.; Wang, P.; Liang, Y.-C.; and Kim, D. I. 2019. Applications of deep reinforcement learning in communications and networking: A survey. *IEEE Communications Surveys & Tutorials*.
- Maeder, A. J.; and Fookes, C. B. 2003. A visual attention approach to personal identification.
- Majaranta, P.; and Bulling, A. 2014. Eye tracking and eye-based human–computer interaction. In *Advances in physiological computing*, 39–65. Springer.
- Marshall, S. P. 2007. Identifying cognitive state from eye metrics. *Aviation, space, and environmental medicine* 78(5): B165–B175.
- Matthews, G.; Middleton, W.; Gilmartin, B.; and Bullimore, M. 1991. Pupillary diameter and cognitive load. *Journal of Psychophysiology*.
- McCamy, M. B.; Otero-Millan, J.; Di Stasi, L. L.; Macknik, S. L.; and Martinez-Conde, S. 2014. Highly informative natural scene regions increase microsaccade production during visual scanning. *Journal of neuroscience* 34(8): 2956–2966.
- McSherry, F. D. 2009. Privacy integrated queries: an extensible platform for privacy-preserving data analysis. In *Proceedings of the 2009 ACM SIGMOD International Conference on Management of data*, 19–30.
- Mnih, V.; Kavukcuoglu, K.; Silver, D.; Rusu, A. A.; Veness, J.; Bellemare, M. G.; Graves, A.; Hiedmiller, M.; Fidjeland, A. K.; Ostrovski, G.; et al. 2015. Human-level control through deep reinforcement learning. *Nature* 518(7540): 529.
- Otero-Millan, J.; Troncoso, X. G.; Macknik, S. L.; Serrano-Pedraza, I.; and Martinez-Conde, S. 2008. Saccades and microsaccades during visual fixation, exploration, and search: foundations for a common saccadic generator. *Journal of vision* 8(14): 21–21.
- Pyrgelis, A.; Troncoso, C.; and De Cristofaro, E. 2017. Knock knock, who’s there? Membership inference on aggregate location data. *arXiv preprint arXiv:1708.06145*.
- Rastogi, V.; and Nath, S. 2010. Differentially private aggregation of distributed time-series with transformation and encryption. In *Proceedings of the 2010 ACM SIGMOD International Conference on Management of data*, 735–746.
- Sammaknejad, N.; Pouretmad, H.; Eslahchi, C.; Salahrad, A.; and Alinejad, A. 2017. Gender classification based on eye movements: A processing effect during passive face viewing. *Advances in cognitive psychology* 13(3): 232.
- Sarathy, R.; and Muralidhar, K. 2011. Evaluating Laplace noise addition to satisfy differential privacy for numeric data. *Trans. Data Priv.* 4(1): 1–17.
- Steil, J.; and Bulling, A. 2015. Discovery of everyday human activities from long-term visual behaviour using topic models. In *Proceedings of the 2015 ACM International Joint Conference on Pervasive and Ubiquitous Computing*, 75–85. ACM.
- Steil, J.; Hagestedt, I.; Huang, M. X.; and Bulling, A. 2019a. Privacy-aware eye tracking using differential privacy. In *Proceedings of the 11th ACM Symposium on Eye Tracking Research & Applications*, 27. ACM.
- Steil, J.; Koelle, M.; Heuten, W.; Boll, S.; and Bulling, A. 2019b. Privaceye: privacy-preserving head-mounted eye tracking using egocentric scene image and eye movement features. In *Proceedings of the 11th ACM Symposium on Eye Tracking Research & Applications*, 26. ACM.
- Stellmach, S.; and Dachselt, R. 2012. Look & touch: gaze-supported target acquisition. In *Proceedings of the SIGCHI Conference on Human Factors in Computing Systems*, 2981–2990. ACM.
- Zhang, Y.; Hu, W.; Xu, W.; Chou, C. T.; and Hu, J. 2018. Continuous authentication using eye movement response of implicit visual stimuli. *Proceedings of the ACM on Interactive, Mobile, Wearable and Ubiquitous Technologies* 1(4): 177.
- Zhao, J.; Zhang, J.; and Poor, H. V. 2017. Dependent Differential Privacy for Correlated Data. In *2017 IEEE Globecom Workshops (GC Wkshps)*, 1–7.